Evaluation of the added mass effect of nonlinear rotational inertial mechanisms in single-degree-of-freedom structures

A. T. Sarkar & N. E. Wierschem
Department of Civil and Environmental Engineering, University of Tennessee, Knoxville, TN, USA

ABSTRACT: Rotational inertial mechanisms have become attractive for structural control applications due to their ability to provide large inertial mass with a small physical mass. Typically, this is done by converting translational motion into the rotation of a flywheel. The inerter, a common rotational inertial mechanism, produces a force proportional to the relative acceleration between the mechanism's terminals. The inerter can provide a constant added mass effect and does not affect the linearity of the system to which it is attached. On the contrary, a nonlinear rotational inertial mechanism produces a force that is a nonlinear function of the mechanism's motion and may vary depending on several factors, including the flywheel velocity, the relative displacement between the terminals, or the hysteresis of the mechanism. As nonlinearities related to the mass of a system have received little attention, it is unclear how nonlinear rotational inertial mechanisms will affect the underlying system's properties and responses. This work investigates the added mass effects provided by a cubic nonlinear rotational inertial mechanism when installed in a single-degree-of-freedom system subjected to forced excitation. The analysis in this paper uses numerical simulations as well as the harmonic balance method to produce approximate analytical results. This study demonstrates that the nonlinear rotational mechanism considered can significantly shift the instantaneous natural frequency and apparent resonance frequency of a structure and provide beneficial modifications to a structure's frequency response behavior.

1 INTRODUCTION

Passive vibration control strategies have been extensively applied in civil engineering to mitigate the effects of dynamic loads, such as wind, seismic ground excitation, and machinery loads (Spencer & Nagarajaiah, 2003). Recently, rotational inertia supplements have gained popularity as a part of passive control devices since the inerter was proposed (Smith, 2002). The inerter is a common feature of rotational inertia supplements, converting translational motion to a flywheel's rotational motion. It is a mechanical element connecting two terminals and produces a large rotational inertia mass while utilizing only a small physical mass. Various inerter-based devices have shown improvement in the dynamic performance of general structural systems, tuned mass damper systems, and base isolation systems (Hwang et al., 2007; Ikago et al., 2012; Lazar et al., 2014).

The inerters used in the previous studies have typically adopted a linear model and configuration. Although inerters have been used in nonlinear systems (Zhang et al., 2019), studies considering nonlinearities related to the rotational inertia mechanism are rare. That being said, in recent years, researchers have explored the effect of nonlinearity resulting from the geometric arrangement of inerters. The work revealed that the addition of the nonlinear inertance mechanism reduces peak force and displacement transmissibility, depending on the frequency range and amplitude of the excitation in comparison to a traditional spring-mass-damper and spring-mass-damper-inerter in a linear arrangement (Moraes et al., 2018; Yang et al., 2020).

Nonlinear rotational inertial mechanisms can be configured such that the inertance of the device varies significantly depending on the device's response, including the relative displacement of the device or the flywheel's rotational velocity. The large variable inertance can cause significant passive changes to the dynamics of the system that it is mounted to, which has the potential to be utilized in vibration control strategies.

This paper investigates the effect of nonlinear inertance on a single-degree-of-freedom (SDOF) mass-spring-damper system. The steady-state response under harmonic excitation is obtained using an analytical approximation based on the harmonic balance method (HBM) and validated by numerical integration. Comparisons of the spring-mass-damper-nonlinear rotational inertial system's performance are made to the traditional spring-mass-damper and spring-mass-damper-inerter system considering force transmissibility and the instantaneous natural frequency of the system.

2 NONLINEAR ROTATIONAL INERTIA MODEL AND FORMULATION

The system considered in this work is depicted in Figure 1, which consists of a one-degree-of-freedom traditional spring-mass-damper system attached to a nonlinear (cubic) rotational inertial mechanism. The nonlinear rotational inertial mechanism with inertance b_{NL} is introduced between the rigid mass m_1 and the base and is

parallel with a spring with stiffness k_1 and a damper with viscous damping coefficient c_1. The mass is subjected to a harmonic loading with amplitude f_e and frequency ω. The equation of motion for the system is

$$m\ddot{x} + b_{NL}\ddot{x}^3 + c\dot{x} + kx = f_e \sin \omega t \quad (1)$$

The cubic relationship between the relative acceleration and forced used for the nonlinear rotational inertial mechanism is not based on a particular physical phenomenon; instead, this type of nonlinearity is assumed for the fundamental investigation of the potential for nonlinear inertance to affect dynamic systems, which is the focus of this work.

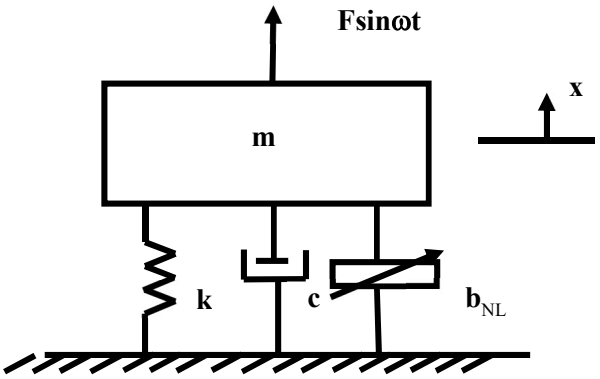

Figure 1. Schematic representation of a SDOF system with a nonlinear rotational inertial mechanism

When $b_{NL}=0$, the system behaves such as a traditional spring-mass-damper (linear) system. Therefore, the traditional mass-spring-damper is treated as a reference when analyzing the performance. Substitution into Eq. (1) can be made with the non-dimensional parameters

$\omega_0 = \sqrt{\frac{k_L}{m}}$, the natural frequency of the system,

$\tau = \omega_0 t$, the non-dimensional time,

$X' = \frac{\dot{x}}{\omega_0}$, the non-dimensional velocity,

$X'' = \frac{\ddot{x}}{\omega_0^2}$, the non-dimensional acceleration,

$F_e = \frac{f_e}{k_L}$, the non-dimensional excitation amplitude,

$\Omega = \frac{\omega}{\omega_0}$, the normalized excitation frequency

$\xi = \frac{c}{2m\omega_0}$, the damping ratio,

and $\eta = \frac{b}{m}\omega_0^4 = \frac{b}{m}.\left(\frac{k_L}{m}\right)^2$, the inertance ratio. The resulting simplified non-dimensional governing equation for this system is

$$X'' + \eta X''^3 + 2\xi X' + X = F_e \sin \Omega t \quad (2)$$

3 FREQUENCY RESPONSE

3.1 *Harmonic Balance Method (HBM)*

In this section, the equation of motion is analyzed using the HBM. The system's response is assumed to be, $X = A\sin(\Omega\tau + \phi) = A\sin\theta$, where A and ϕ are the response amplitude and phase angle, respectively. Substituting the assumed harmonic displacement response into Eq. (2) yields

$$-\Omega^2 A\sin\theta - \eta\Omega^6 A^3 \sin^3\theta + 2\xi\Omega A\cos\theta + A\sin\theta = F_e \sin(\theta - \phi)\tau \quad (3)$$

By omitting the higher-order harmonic terms and applying trigonometric relationships, Eq. (3) becomes

$$-\Omega^2 A\sin\theta - \eta\Omega^6 A^3 \tfrac{3}{4}\sin\theta + 2\xi\Omega A\cos\theta + A\sin\theta = F_e\sin\theta\cos\phi - F_e\cos\theta\sin\phi \quad (4)$$

Balancing the coefficient of cosθ and sinθ on both sides, we obtain

$$-\Omega^2 A - \tfrac{3}{4}\eta\Omega^6 A^3 + A = F_e\cos\phi \quad (5)$$

$$2\xi\Omega A = -F_e\sin\phi \quad (6)$$

Eliminating ϕ in Eq. (5) and Eq. (6), the relationship between the response amplitude and the normalized excitation frequency becomes

$$\tfrac{9}{16}\eta^2\Omega^{12}A^6 - \tfrac{3}{2}\left(1-\Omega^2\right)\eta\Omega^6 A^4 + \left[\left(1-\Omega^2\right)^2 + 4\xi^2\Omega^2\right]A^2 = F_e^2 \quad (7)$$

3.2 *Numerical Validation*

The Runge-Kutta numerical integration technique simulates the time history response, and the steady-state vibration amplitude is extracted from that. For this analysis, the system parameters are set as η=10 and, ζ=0.025. Additionally, two forcing amplitudes, F_e=0.05 and 0.2, are considered.

Figure 2 presents the frequency response curve for the nonlinear system by the HBM and the Runge-Kutta method. Both the analytical and numerical curves correspond well. However, in the numerical analysis, a 'jump' phenomenon is observed due to multivalued amplitudes in the curve's bending. The bending behavior observed in the curve is similar to the harmonically excited nonlinear energy sink with softening stiffness. It also shows that as excitation amplitude increases, the maximum response amplitude that can be stably achieved

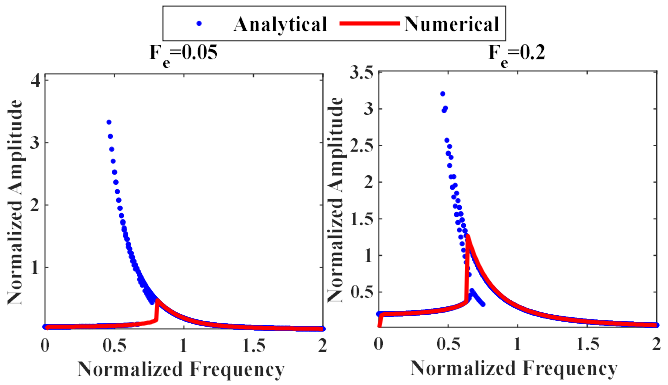

Figure 2. Frequency response curves for different normalized forcing amplitudes 0.05 (left) and 0.2 (right)

with the numerical solution increases, and the frequency with the maximum response, which can be referred to as a pseudo resonance frequency, decreases.

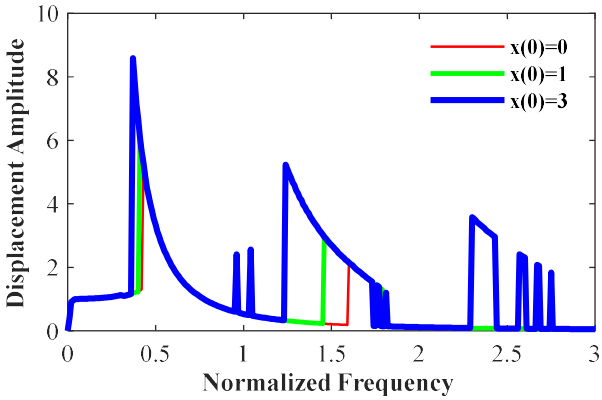

Figure 3. Frequency response curves of damped nonlinear system with different initial conditions

Figure 3 presents the numerical frequency response curves of the damped nonlinear system with different initial conditions. The analysis is performed for a forcing amplitude of 1 and changes in the initial displacement. Higher initial energy produces more mass effects and shifts the frequency response curve to higher steady-state amplitudes and lower frequencies. This contrasts with the behavior of a linear system in which the amplitude of the steady-state response is proportional to the amplitude of the excitation and does not depend on the initial conditions. Moreover, superharmonic pseudo resonance cases become more evident as the initial displacement increases. These jumps cannot be captured analytically with the HBM due to eliminating higher-order harmonics in the frequency response representation. It is found that the superharmonic pseudo resonance responses show continuous 'jump' at frequencies where multiple solutions exist for higher initial displacement. This happens in multiple steady-state solutions when the numerical solver determines the moderate-values corresponding to saddle points. These saddle points are difficult to realize physically due to their unstable nature.

4 FORCE TRANSMISSIBILITY

The performance of the nonlinear rotational inertia device can be evaluated using force transmissibility, which is the ratio of the force transmitted to a rigid base to the excitation force at a given forcing frequency. The non-dimensional magnitude of the applied force is $\hat{F}_e = 0.1$. Thus, the magnitude of force transmissibility can be measured using the equation below,

$$|T| = \left(\sqrt{\left(-\Omega^2 A - \tfrac{3}{4}\eta\Omega^6 A^3 + A\right)^2 + \left(2\zeta\Omega A\right)^2} \right) / F_e \qquad (8)$$

Figure 4 compares the force transmissibility of the nonlinear rotational inertia system and spring-mass-damper-inerter system for ζ=0.025 and F_e=0.1. The inertance ratios for both nonlinear and linear systems are set at 10 for this analysis. It shows that the maximum response of the nonlinear rotational inertia system occurs at a lower frequency compared to the spring-mass-damper-inerter system. Due to unstable solutions in the nonlinear system analysis, the peak force transmissibility cannot be identified. Bifurcation analysis will be carried out in the future to determine the peak force transmissibility. At higher frequencies, all the curves reach a plateau. However, this plateau is much lower in amplitude for the nonlinear curve; thus, allowing for more effective isolation of high frequencies. The addition of the nonlinear rotational inertia mechanism reduces overall force transmission. This mechanism can be a matter of interest for structural control applications in that it may simultaneously reduce response and provide better higher frequency isolation.

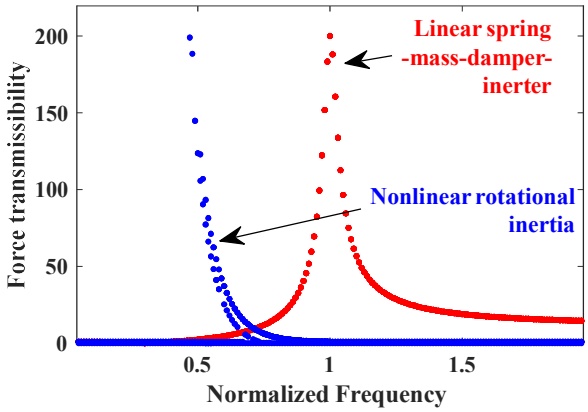

Figure 4. Force transmissibility characteristics of nonlinear rotational inertial mechanism and spring-mass-damper-inerter system (η=10, ζ=0.025 and F_e=0.1)

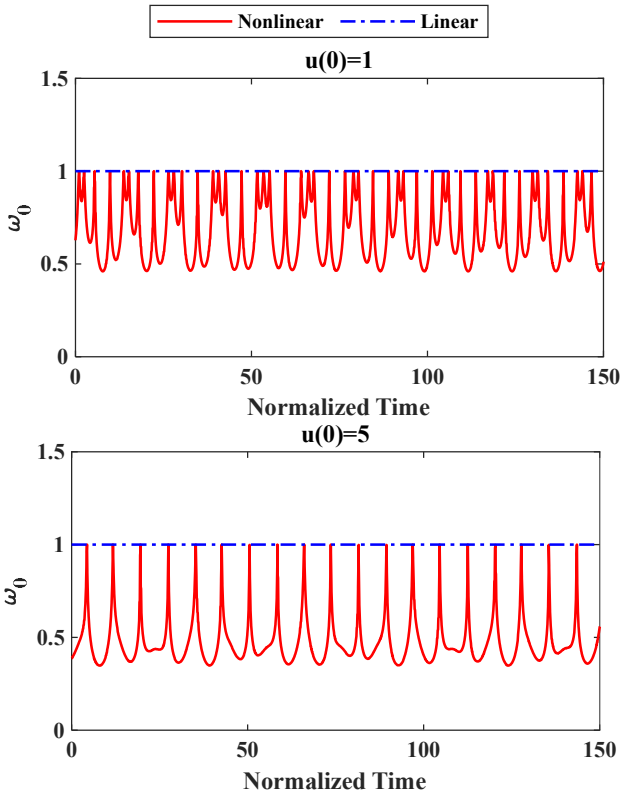

Figure 5. Instantaneous natural frequency comparison for different initial displacements 1 (top) and 5 (bottom)

5 TIME HISTORY RESPONSE

For this analysis, the system parameters are set as η=10 ζ=0, and F_e=1. Figure *5* shows the instantaneous natural frequency obtained numerically for different non-dimensional initial displacements (1 and 5). The natural frequencies are obtained by an Eigenvalue analysis at each time step considering the mass effects provided by the nonlinear rotational inertial mechanism at that time step.

The dash-dot line represents the natural frequency of the mass-spring-damper system; it remains the same for all time histories. However, for the nonlinear system, the mass effect provided by the nonlinear rotational inertial mechanism is constantly changing. Thus, the natural frequency is changing throughout the time-history of the response. For higher energy input, higher shifts in natural frequency are feasible.

6 CONCLUSIONS

This paper investigates the dynamic behavior of a cubic nonlinear rotational inertia mechanism in a SDOF mass-spring-damper system. Linear inerters have been incorporated in systems that have shown effectiveness in reducing the response of the structure; however, nonlinear rotational inertia mechanisms have not received much previous consideration. The frequency response relationship is obtained using the harmonic balance method. Additionally, force transmissibility was used as an index to measure the performance of vibration isolation. Numerical simulations were performed following the Runge-Kutta technique to validate the analytical outcomes.

The results of this study show that the presence of the nonlinear rotational inertial mechanism can reduce the dominant frequency and force transmissibility as well as the addition of higher frequency dynamics. The study reveals that the added mass effect provided by the cubic rotational inertial mechanism continually changes and is dependent on the initial conditions of the system and the amplitude of the excitation. Overall, the study suggests that the nonlinear rotational inertial mechanisms can provide a beneficial effect in passive vibration control. Although a physically realistic device has not been proposed for a cubic nonlinear rotational inertial mechanism, the findings of this study can help to improve the general understanding of the dynamic properties of nonlinear rotational inertial attachments for vibration mitigation.

ACKNOWLEDGMENT

This research was supported in part by the National Science Foundation (NSF) under Grant No. CMMI-1944513. The findings, opinions, recommendations, and conclusions in this paper are those of the authors alone and do not necessarily reflect the views of others, including the sponsors.

REFERENCES

Hwang, J.-S., Kim, J., & Kim, Y.-M. 2007. Rotational inertia dampers with toggle bracing for vibration control of a building structure. *Engineering Structures*, *29*(6), 1201–1208.

Ikago, K., Saito, K., & Inoue, N. 2012. Seismic control of single-degree-of-freedom structure using tuned viscous mass damper: THE TUNED VISCOUS MASS DAMPER. *Earthquake Engineering & Structural Dynamics*, *41*(3), 453–474.

Lazar, I. F., Neild, S. A., & Wagg, D. J. 2014. Using an inerter-based device for structural vibration suppression: USING AN INERTER-BASED DEVICE FOR STRUCTURAL VIBRATION SUPPRESSION. *Earthquake Engineering & Structural Dynamics*, *43*(8), 1129–1147.

Moraes, F. de H., Silveira, M., & Gonçalves, P. J. P. 2018. On the dynamics of a vibration isolator with geometrically nonlinear inerter. *Nonlinear Dynamics*, *93*(3), 1325–1340.

Smith, M. C. (2002). Synthesis of mechanical networks: The inerter. *IEEE Transactions on Automatic Control*, *47*(10), 1648–1662.

Spencer, B. F., & Nagarajaiah, S. 2003. State of the Art of Structural Control. *Journal of Structural Engineering*, *129*(7), 845–856.

Yang, J., Jiang, J. Z., & Neild, S. A. 2020. Dynamic analysis and performance evaluation of nonlinear inerter-based vibration isolators. *Nonlinear Dynamics*, *99*(3), 1823–1839.

Zhang, Z., Lu, Z.-Q., Ding, H., & Chen, L.-Q. 2019. An inertial nonlinear energy sink. *Journal of Sound and Vibration*, *450*, 199–213.